Oscillatory Thermocapillary Flow in Cylindrical Columns of High Prandtl Number Fluids

Kyu-Jung Lee*
Department of Mechanical Engineering, Korea University
Yasuhiro Kamotani, Simon Ostrach
Department of Mechanical and Aerospace Engineering, Case Western Reserve University

Oscillatory thermocapillary flow of high Prandtl number fluids in the half-zone configuration is investigated. Based on experimental observations, one oscillation cycle consists of an active period where the surface flow is strong and the hot corner region is extended and a slow period where the opposite occurs. It is found that during oscillations the deformation of free surface plays an important role and a surface deformation parameter S correlates the experimental data well on the onset of oscillations. A scaling analysis is performed to analyze the basic steady flow in the parametric ranges of previous ground-based experiments and shows that the flow is viscous dominant and is mainly driven in the hot corner. The predicted scaling laws agree well with the numerical results. It is postulated that the oscillations are caused by a time lag between the surface and return flows. A deformation parameter S represents the response time of the return flow to the surface flow.

Key Words: Oscillatory Thermocapillary Flow, Scaling Analysis, Half Zone Configuration, High Prandtl Number Fluid, Surface Deformation

Nomenclature

Ar : Aspect ratio
Bd : Dynamic Bond number
Bo : Static Bond number
$D(R)$: The column diameter (radius)
g : The gravitational acceleration,
Gr : Grashof number
L : Length of the liquid column
Ma : Marangoni number
Nu : Nusselt number
p : Pressure
Pr : Prandtl number
r, z : Radial and axial coordinate
$R\sigma$: Surface tension Reynolds number
S : Surface deformation parameter
T : Temperature
t : Time
u, v : Axial and radial velocity
$U_0, \overline{U}_0$: Characteristic velocity

Greeks

α : Thermal diffusivity
β : Volumetric expansion coefficient
Δ, δ : Characteristic length in hot (cold) corner region
δ_s : Thickness of surface deformation
ΔT : Imposed temperature difference
μ : Fluid viscosity
ν : Kinematic viscosity
ρ : Fluid density
σ : The surface tension.
σ_T : Temperature coefficient of surface tension ($=\partial\sigma/\partial T$)

Subscripts

Cr : Critical
H : Hot
C : Cold

* Corresponding Author,
E-mail : kjlee@korea.ac.kr
TEL : +82-2-3290-3359; **FAX** : +82-2-928-9768
Department of Mechanical Engineering, Korea University, 5-1, Anam-dong, Sungbuk-ku, Seoul 136-701, Korea.(Manuscript **Received** October 2, 2000; **Revised** February 26, 2001)

1. Introduction

Variations in surface tension due to temperature variations along a liquid free surface generate thermocapillary flows. Much attention has been given over the past 30 years to the theoretical, experimental, and numerical analyses of thermocapillary flow for the various configurations. One important feature of thermocapillary flows found in previous experiments is a transition from steady to oscillatory (time-periodic) flow under certain conditions. The phenomenon was originally discovered by Schwabe et al. (1978) and Chun and Wuest (1979) in the so-called half-zone simulation of the floating zone crystal growth process in which a cylindrical liquid column is suspended between two differently heated rods. Since the oscillation phenomena not only are interesting scientifically but also have significant implications in many practical applications, it has been studied in more detail in the subsequent half-zone experiments by several investigators (Chun, 1980; Schwabe et al., 1982, 1990; Preisser et al., 1983; Kamotani et al., 1984; Ostrach et al., 1985; Kamotani and Lee, 1989; Velten et al., 1991; Lee et al., 1995). In those experiments the liquid column diameters were made small (less than 1 cm) to minimize the effects of buoyancy and gravity. Although the test configuration was meant to simulate crystal growth of low Prandtl number ($Pr<1$) crystal melts, high Pr (>1) fluids were used in the past tests for experimental simplicity.

Despite all the work in the past the oscillatory thermocapillary flow phenomenon is not yet fully understood. Questions still remain concerning the physical mechanism of oscillations and the parameter(s) defining their onset. Experimentally for a given test fluid and zone dimensions the flow becomes oscillatory beyond a certain critical temperature difference across the column length. From dimensional analysis of thermocapillary flows (Ostrach, 1977), it can be shown that the only parameter that contains the temperature difference is the Marangoni number (Ma) if the liquid free surface is assumed to be undeformable. Therefore, it was assumed by many investigators that the transition condition is characterized by a critical Marangoni number (Ma_{cr}). Previous ground-based experiments suggest that Ma_{cr} is around 10^4 for high Pr fluids. However, the Ma in previous experiments were limited to be of order 10^4 or less due to the limitation of available fluids and gravity effect on earth. In experiments under micro-gravity environment (Napolitano et al., 1986; Monti and Fortezza, 1991) the oscillatory flow was observed at much larger Ma than observed on earth.

Clearly, the use of Ma_{cr} to characterize the onset of oscillations is not definitive. Furthermore, Kamotani et al. (1984) and Ostrach et al. (1985) measured the critical temperature difference by systematically changing the column diameter and length and also found that Ma alone cannot specify the transition. That necessitated an additional parameter containing the temperature difference. The need for an additional parameter to correlate the oscillatory flow data was the first indication that surface deformations, in some way, played a role in the oscillatory phenomena. Based on their data, Kamotani et al. (1984) proposed a surface deformation parameter to specify the transition for high Pr fluids. The idea behind the parameter was that the free surface deformation caused by the flow, albeit very small, changes the flow response time by a significant amount so that it triggers a three-way coupling among the velocity and temperature fields and the surface deformation. An analysis of the surface deformation effect is the main objective of the present work. Lai (1990) and Chen et al. (1991) showed the existence of a time lag between the surface and return flows in unsteady thermocapillary flow caused by a deformable free surface. Monti (1987) proposed a modified Weber number, which represents the flexibility of the free surface, to correlate microgravity data on the onset of oscillations.

Theoretically the appearance of oscillatory flow in the half-zone configuration has been treated as a convective instability with a nondeformable free surface. Xu and Davis (1984) analyzed the stability of the shear flow, which was

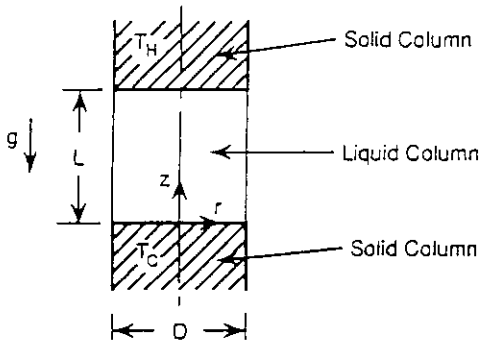

Fig. 1 Schematic of half-zone configuration

assumed to exist in the core region (away from the end walls) of a long float zone with a linear surface temperature variation driving the flow. Beyond a Matangoni number propagating hydrothermal waves appear, resulting in temperature oscillations at a given point. Shen et al. (1990) applied the energy method to the numerically computed basic flow field in a half-zone to determine conditions for stability with respect to arbitrary axisymmetric disturbances. In their analyses the stability criterion is very sensitive to the value of a coupling parameter, which joins the velocity and temperature disturbances to form generalized disturbance energy. Attempts have been made to simulate the oscillation phenomenon by numerical analysis (Rupp et al., 1989; Chen and Chin, 1995; Wanschura et al., 1995; Chen and Hu, 1998). Since the free surface was assumed to be undeformable in all of the above analyses, the onset of oscillations was not well supported by experimental evidence.

In the present work the importance of a deformable free surface on the oscillation phenomenon is examined. The physical mechanism of oscillations is delineated based on the information obtained from experiments and a numerical analysis and the surface deformation parameter proposed earlier is formally derived. Since much information is available on the phenomenon in the half-zone configuration with high Pr fluids, we focus our attention on that configuration herein.

2. Oscillatory Flow in Half-Zone

The half-zone configuration investigated herein is sketched in Fig. 1. A vertical liquid bridge is formed between two cylindrical metal rods. By heating the upper rod thermocapillary flow is generated while minimizing buoyancy effects. If the liquid free surface is assumed to be flat and undeformable, the important dimensionless parameters for steady flow (Ostrach, 1977) are Prandtl number ($Pr=\nu/\alpha$), surface tension Reynolds number ($R\sigma=\sigma_T\Delta TL/\mu\nu$), Grashof number ($Gr=g\beta\Delta TL^3/\nu^2$), and aspect ratio ($Ar = L/D = L/2R$). The Marangoni number is defined as $Ma=R\sigma Pr$. The ratio of buoyancy to thermocapillary forces is represented by $Gr/R\sigma$, which is called the dynamic Bond number (Bd). The liquid column cannot be exactly cylindrical in one-g because of hydrostatic pressure and its shape is determined by the liquid volume, aspect ratio, and the static Bond number which is defined as $Bo=\rho gL^2/\sigma$.

Before the appearance of oscillations the flow is axisymmetric and recirculates in a toroidal pattern with the fluid moving from the hot to cold end along the free surface. Once the imposed ΔT reaches a critical value (ΔT_{cr}), the flow suddenly becomes three-dimensional and both the fluid motion and the temperature oscillate temporally and spatially. If the above listed parameters are the only important ones, the ΔT_{cr} should be non-dimensionalized as Ma_{cr} (or $R\sigma_{cr}$) in the absence of gravity and for a given fluid (or Pr) Ma_{cr} should be a function of Ar only. Figure 2 (a) shows Ma_{cr} vs. Ar measured with various column diameters using 2 cs silicone oil ($Pr=27$). It is very clear that Ma_{cr} does not correlate the data and thus it is not the appropriate parameter to represent the onset of oscillations. Another parameter containing ΔT is needed. After analyzing the data obtained under the various conditions and the physical mechanism of oscillations, Kamotani et al. (1984) proposed a parameter called the surface deformation parameter (or S parameter) that is defined as $S=(1/Pr)(\sigma_T\Delta T/\sigma)$. Note that S does not contain

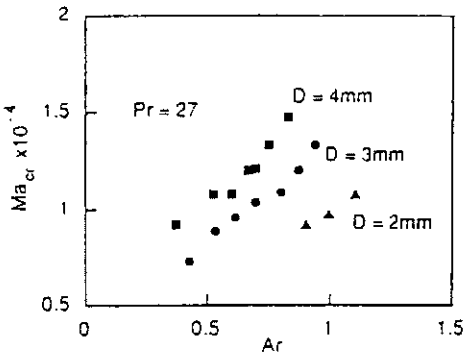

(a) Ma_{cr} vs. Ar

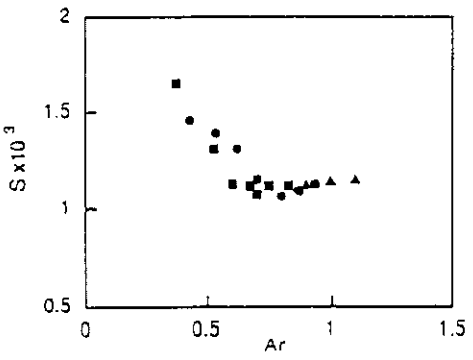

(b) S vs. Ar

Fig. 2 Critical condition for onset of oscillations

(a)

(b)

(a → b)

Fig. 3 Cross-sectional views of flow during oscillations

any zone dimension and is essentially a modified capillary number. Figure 2(b) shows that the onset conditions can be correlated by S alone and in the range $Ar>0.7$ the oscillations occur if S is larger than about 1.1×10^{-3}. The data taken with other fluids (Ostrach et al., 1985) gave the critical S values close to the above value. The S parameter is considered to represent the effect of surface deformation as will be discussed in detail in Sec. 4.

In order to gain some insight into the physical mechanism of oscillations the oscillatory flow and temperature fields were investigated experimentally. The flow field was studied by flow visualization. A small amount of alumina particles (1-20 μm dia.) was added to the test fluid and illuminated by a laser light sheet. Figure 3 shows two photographs of the flow structure in a cross-sectional plane taken at two different times for $Ar=0.625$. During oscillations a non-axisymmetric flow pattern travels around the zone and the pattern varies in a periodic manner in the azimuthal direction as described by Preisser et al. (1983). The second picture was taken when the pattern in the first figure rotated just 180°, so the two pictures are mirror images of each other. We focus our attention on the right half of the zone in Fig. 3. In Fig. 3(a) one sees a strong motion toward the free surface near the top hot wall and the location of the cell center, which is closer to the cold wall than the one in the left half, indicates the flow along the free surface is also strong. We call this period the active period. In Fig. 3(b) one sees that the strong motion originating from the free surface region near the cold wall does not return to the hot region in the right half and the cell center location indicates the motion near the hot region is relatively weak and confined in a small region. This period is called the slow period. Thus the flow goes through an active and a slow period in one cycle in one radial plane.

Other useful information on the flow was

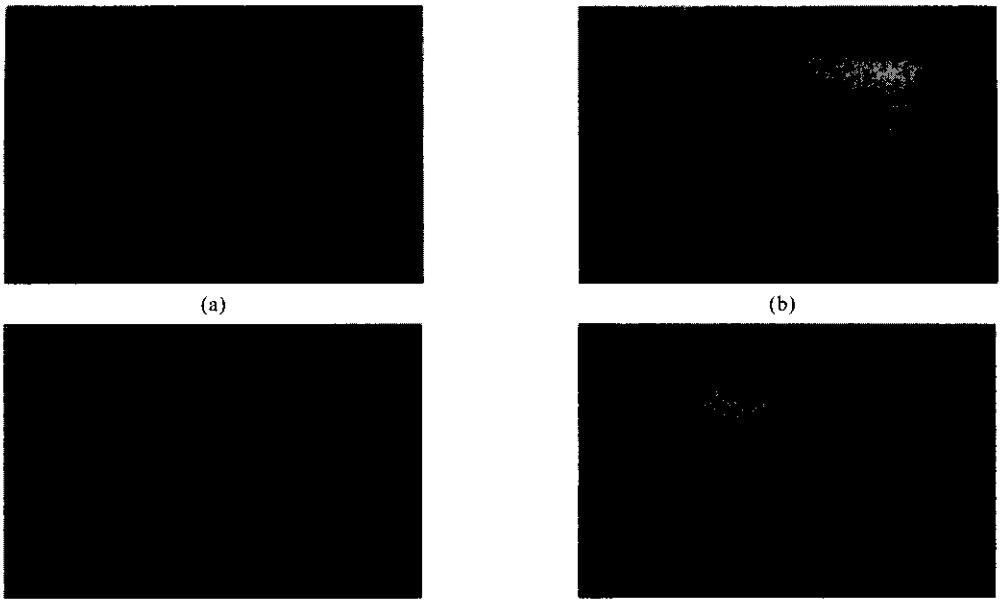

Fig. 4 Infrared images of free surface during oscillations

obtained by scanning the free surface with an infrared imager (Inframetrics Model 600). The instrument scans the surface at 30 frames per second and measures the radiation emitted from the surface in the 8-14 μm wavelength range. To be more precise, it detects radiation emitted by a thin layer (less than 0.2mm thick in the case of silicone oils) adjacent to the free surface. The infrared images of a silicone oil (2 cs) zone taken at four different times in one cycle of oscillation are presented in Fig. 4. In Fig. 4(a) the hot region, represented by red and yellow colors, is confined to a small region near the hot wall and this corresponds to the slow period. In Fig. 4(b) a larger hot region appears on the right indicating a beginning of the active period during which convection along the free surface is strong. In Fig. 4(c) the active period covers the full view and then moves to the left in Fig. 4(d). Therefore, the information from the infrared images seems to be consistent with our concept of cyclic active-slow period obtained from the flow visualization and this information will be used to explain the physical mechanism of oscillations in Sec. 4.

3. Analysis of Basic Flow Field

Before we discuss the oscillation mechanism it is useful to understand the basic steady flow. A scaling analysis of the steady thermocapillary flow in the half-zone is presented herein to determine what forces are important in the flow and to derive the important velocity and length scales. Since detailed experimental data is very limited, a numerical analysis is also performed to check the scaling laws as well as to give some guidance to the scaling analysis. The analysis is limited to the conditions under which the previous oscillatory thermocapillary flow experiments were performed, namely $Pr=10\sim100$, $Ar=0.35\sim1.0$, $Ma<2.5\times10^4$. The effects of buoyancy and radiation are not considered. The free surface is assumed to be flat and rigid in this steady flow analysis. The numerical analysis is based on the SIMPLER algorithm by Patanker (1980). Based on the earlier analyses (Zebib et al., 1985; Carpenter and Homsy, 1990), non-uniform grid systems were adopted with meshes graded toward the hot and cold walls and toward the free sur-

Ar=0.625
ΔT=7℃
R_σ=350
Ma=9250
Gr=290
Pr=26.5

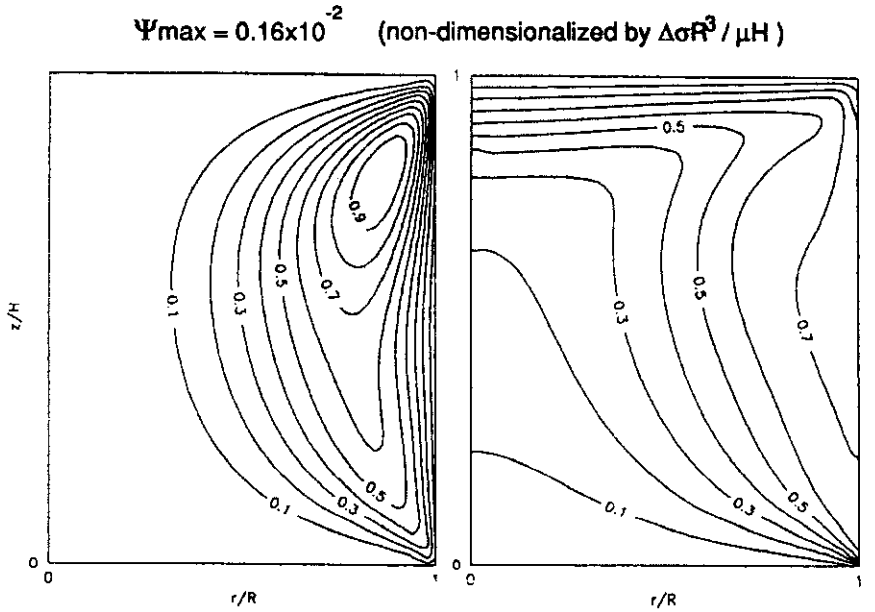

(a) Streamline pattern (b) Isotherm Profile

Fig. 5 Computed streamlines and isotherms

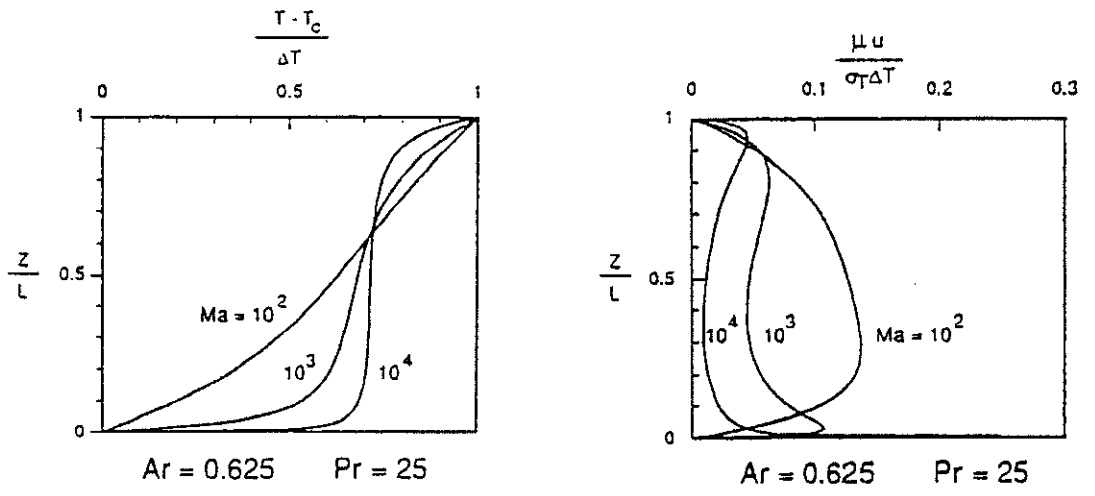

(a) Surface temperature distributions (b) Surface velocity distributions

Fig. 6 Surface temperature and velocity distribution

face. The finest grid system used was 68×60 (axial x radial) with the smallest spacing of 0.004.

Shown in Fig. 5 are the computed streamline and isotherm patterns for a typical condition. The

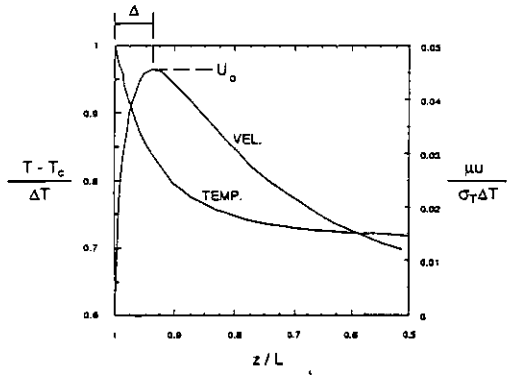

Fig. 7 Surface velocity and temperature distributions near hot corner region

flow along the free surface (herein called the surface flow) is confined to a relatively narrow region near the surface and the interior flow back to the hot region (called the return flow) is much slower. The trend of computed flow pattern agrees well with experimental observations. The isotherms indicate strong effects of convection and the temperature along the free surface is relatively uniform over a large part of the surface.

The surface temperature distribution is important because it is directly related to the driving force of the flow. The computed surface temperature and velocity distributions are presented in Fig. 6 for three different values of Ma. With increasing Ma, convection causes large surface temperature changes near the hot and cold walls with a relatively uniform temperature region in between. As a consequence, the driving force exists mainly in those corner regions and the velocity has a peak in each of those regions. Since oscillatory flow appears at high Ma, it is important to understand what is happening in those corner regions.

In the hot corner the important quantities are the location of the velocity peak Δ(see Fig. 7), which represents the extent of the hot corner region, and the peak velocity value U_o that represents the characteristic velocity in that region. A scaling analysis is performed to determine how those quantities vary with Ma, Ar, and Pr.

Before the scaling analysis, the importance of inertia forces relative to viscous forces in the flow needs to be discussed. The ratio of those two forces is represented by $R\sigma$, which is larger than unity for the conditions under which the onset of oscillations has been observed. For example, with 2 cs silicone oil (Pr=27), D=3mm, and L=2.1 mm, ΔT(maximum temperature difference for steady flow) was measured to be 7.2℃, which gives $Ma=1.0\times10^4$ and $R\sigma$=370. However, the is based on the velocity scale $\sigma_T\Delta T/\mu$, but in reality U_o is less than 5% of the value when Ma is large as can be seen in Fig. 6. Moreover, since the flow is driven in a relatively small region when Ma is large, the length scale in should also be reduced. Based on the computed values of U_o and Δ, the actual Reynolds number is reduced to a value less than unity (about 0.7) for the above conditions, indicating that the viscous forces are much more important than the value $R\sigma$=370 suggests. The effect of inertia forces is small, but convection heat transfer is very important. Therefore, the flow is assumed to be dominated by viscous forces in the following scaling analysis and thus the important parameters for the flow are Ma and Ar.

The momentum equation in the axial direction without inertia terms is

$$\frac{\partial p}{\partial z}=\mu\left[\frac{\partial^2 u}{\partial z^2}+\frac{1}{r}\frac{\partial}{\partial r}\left(r\frac{\partial u}{\partial r}\right)\right] \tag{1}$$

The energy equation is

$$u\frac{\partial T}{\partial z}+v\frac{\partial T}{\partial r}=a\left[\frac{\partial^2 T}{\partial z^2}+\frac{1}{r}\frac{\partial}{\partial r}\left(r\frac{\partial T}{\partial r}\right)\right] \tag{2}$$

The shear stress condition at the free surface is

$$\mu\frac{\partial u}{\partial r}=\sigma_T\frac{dT}{dz} \tag{3}$$

As mentioned above, the length scale Δ defines the extent of the hot corner region in the axial direction (see Fig. 7). Since the flow is viscous, the momentum equation for the flow contains only two viscous terms and a pressure term. Those two viscous terms are equally important in the corner region where the flow turns. Therefore, by balancing those two viscous terms one finds that the length scale in the radial direction should be the same as that in the axial direction. Using that

fact, the velocity scale U_o can be determined from Eq. (3) as

$$\mu\frac{U_o}{\Delta}\sim\sigma_T\frac{\Delta T_H}{\Delta} \text{ or } U_o\sim\frac{\sigma_T\Delta T_H}{\mu} \tag{4}$$

where ΔT_H is the surface temperature variation over Δ. Since the length scales in the axial and radial directions are the same in the corner region, the continuity equation shows that U_o is the velocity scale in the radial direction as well.

As can be seen in Fig. 7, the surface velocity increases only in the region where the surface temperature changes sharply close to the wall. Although a finite temperature gradient exists beyond , the velocity decreases there. That observation and the analysis of isotherms in Fig. 5(b) suggest that Δ is the region where the conduction of heat from the hot wall is important. This means that Δ scales with the thermal boundary-layer thickness along the hot wall. Along the hot wall the fluid velocity varies from zero (at $r=0$) to U_o (near $r=R$), so the average velocity along the wall scales with U_o and to obtain Δ we balance the conduction term in the axial direction and the convection term in the radial direction in the energy Eq. (2), which gives

$$\Delta^2\sim\frac{\alpha R}{U_o} \tag{5}$$

According to Fig. 5(b) the thermal boundary layer thickness is nearly constant along the hot wall, which suggests that the velocity along the wall varies almost linearly with r from zero to U_o (stagnation-point type flow). Also it can be shown that if the thermal boundary layer thickness is used as the length scale, the ratio of inertia to viscous forces in the momentum equation is represented by $1/Pr$ so that the inertia force is relatively small when Pr is large, which is consistent with the assumption made earlier. In the region outside the hot corner the surface velocity decreases despite of the fact that positive thermocapillary driving force exists there (Fig. 7). The reason for the velocity decrease is that in the case of $Pr>1$ the viscous retardation effect from the hot wall is still important outside the thermal boundary layer (or Δ).

Convection of heat toward the cold wall causes a large temperature gradient near the wall and the surface velocity increases again (Fig. 6). This region is called the cold corner region. In the cold corner the flow is accelerated toward the wall, which squeezes the corner region further. The extent of the cold corner is determined by balancing the surface convection toward the wall and conduction to the opposite direction. From the analysis of the cold corner Ostrach et al. (1985) found that the extent of the region scales with Ma^{-1}, which is much smaller than the hot corner size, and the velocity scales with $\sigma_T\Delta T_c/\mu$ (ΔT_C: surface temperature variation in the cold corner), which is close to the velocity scale in the hot corner. Therefore, the overall mass flux generated in the hot corner is much greater than that generated in the cold corner. Although the temperature gradient at the cold wall is very large in the cold corner, the region is relatively small so that the total heat transfer rate to the cold wall is determined by the thermal boundary layer along the wall beyond the corner region. Since the surface flow convects heat to the cold wall, the heat transfer region at the cold wall should scale with the radial extent of the surface flow as was assumed in the scaling analysis by Zebib et al. (1985). The radial dimension of the surface flow scales with R beyond the hot corner because the flow is viscous and it remains nearly constant (approximately equal to $0.2R$, see Fig. 5) until it is forced to turn due to increased pressure in the cold corner. After the turning the lateral flow extent remains at about $0.2R$ since the flow is viscous dominated. Since the velocities in the hot and cold corners scale closely with $\sigma_T\Delta T/\mu$, the average surface flow velocity ($\overline{U}_o$) over the zone length is considered to scale with the same quantity and just after the turning the velocity scale remains at $\overline{U}_o$ because the flow extent does not change. The flow creates a thermal boundary layer along the cold wall with characteristic thickness δ. When Ma is large, δ is much less than R (or $0.2R$) so that when estimating δ one has to take into account the fact that the velocity close to the wall is less than the velocity $\overline{U}_o$. Including the velocity adjustment the balance of the convection term in the radial direction and

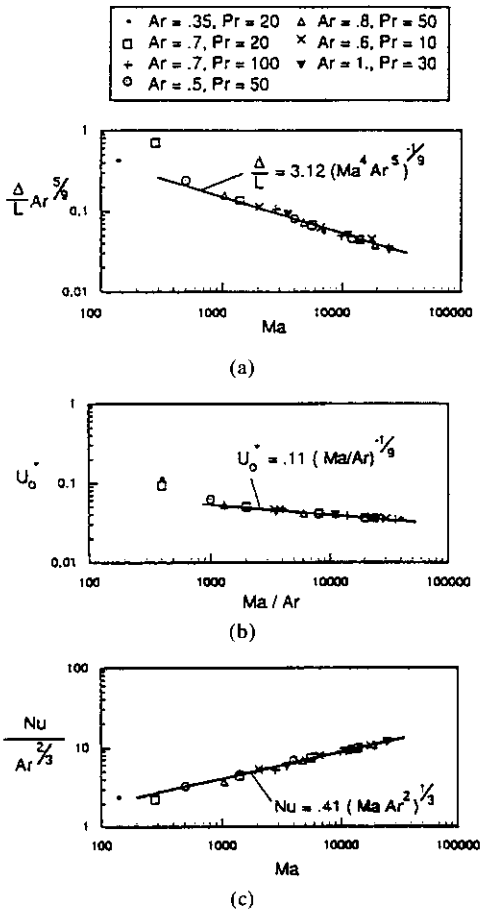

Fig. 8 Comparison of scaling laws with numerical results

the conduction in the axial direction in the energy equation gives

$$\overline{U}_o \frac{\delta}{R}\frac{\Delta T_c'}{R} \sim \alpha \frac{\Delta T_c'}{\delta^2} \tag{6}$$

where $\Delta T_c'$ is the average temperature drop across δ. Along the hot wall the flow accelerates in the flow direction, which makes the thermal boundary layer thickness nearly constant, but along the cold wall the flow decelerates in the flow direction (decreasing r) so that δ increases quickly (Fig. 5).

Based on the definition of Nusselt number (Nu) one obtains

$$Nu \sim \frac{k\frac{\Delta T_c'}{\delta}\pi R^2}{k\frac{\Delta T}{L}\pi R^2} \sim \frac{L}{\delta} \tag{7}$$

where $\Delta T_c'$ is assumed to scale with ΔT as discussed below. And since the total heat transfer rate at the hot wall should be equal to that at the cold wall, one has

$$k\frac{\Delta T_H}{\Delta}\pi R^2 \sim k\frac{\Delta T_c'}{\delta}\pi R^2 \tag{8}$$

When Ma is large, a large temperature drop occurs near the cold wall because of convection along the free surface (Fig. 6). Therefore, one can assume that ΔT_c and $\Delta T_c'$ scale with ΔT when Ma is large. With that assumption Eqs. (4)~(8) give the following scaling laws:

$$U_o^* = \frac{\mu U_o}{\sigma_T \Delta T} \sim \frac{\Delta T_H}{\Delta T} \sim (Ma/Ar)^{-1/9}$$
$$\frac{\Delta}{L} \sim (Ma^4 Ar^5)^{-1/9}$$
$$Nu \sim (MaAr^2)^{1/3} \tag{9}$$

The quantities U_o, Δ, and Nu can be determined by numerical analysis. The scaling laws are compared with the present numerical results obtained under various conditions in Fig. 8. They are in very good agreement in the range of $Ma > 1.5\times10^3$, which suggests that the above scaling analysis and flow structure are correct.

4. Physical Mechanism of Oscillations

One important effect of a flexible free surface is that the pressure at the free surface is determined by the surface curvature in the absence of gravity. When the flow is changed locally by thermocapillarity, there is a time lag before the bulk of the fluid responds to the change because it takes a finite time to change the free surface shape and thus the pressure field. This time lag is the key part of the present concept of oscillations, which was originally discussed in the earlier papers (Kamotani et al., 1984; Ostrach et al., 1985). Assuming that the free surface deformation is small, pressure p at the free surface is related to the radii of curvature of the surface as

$$p = \sigma\left(\frac{1}{R} - \frac{d^2R}{dZ^2}\right) \tag{10}$$

where R is the local radius of the zone. Variation of p occurs mainly in the relatively small driving

force region (Δ), so the second curvature is more important in Eq. (10). Therefore, p near the free surface scales with $\sigma\delta_s/\Delta^2$ where δ_s is the amount of free surface deformation. In order to estimate p (and δ_s) we add the unsteady term $\rho\cdot\partial u/\partial t$ to the momentum Equation. The free surface deformation δ_s occurs in a very short time after the surface velocity is changed, so the unsteady term is more important than the viscous terms in Eq. (1) during the deformation (the ratio of the unsteady to viscous term during the deformation can be shown to be $(U_oL/\nu)(L/\delta_s)$, which is large). The order of magnitude of $\partial u/\partial t$ can be estimated by knowing that the velocity variation over one cycle scales with U_o. Then, by balancing the unsteady term and the pressure gradient in Eq. (1) one gets

$$\rho\frac{U_o}{L/U_o}\sim\sigma\frac{\delta_s}{\Delta^2}\frac{1}{\Delta} \text{ or } \frac{\delta_s}{\Delta}\sim\frac{\rho U_o^2\Delta^2}{\sigma L} \tag{11}$$

For a fixed Ar, R scales with L, so using Eq. (5) the above equation can be written as

$$\frac{\delta_s}{\Delta}\sim\frac{\rho U_o\alpha}{\sigma} \tag{12}$$

It is shown in Sec. 3 that $\mu U_o/\sigma_T\Delta T$ is only a weak function of Ma/Ar. If we neglect the dependence on Ma/Ar and consider $\mu U_o/\sigma_T\Delta T$ to be constant, the above equation reduces to

$$\frac{\delta_s}{\Delta}\sim\frac{1}{Pr}\frac{\sigma_T\Delta T}{\sigma}=S \tag{13}$$

Thus, the S parameter represents the amount of free surface deformation relative to Δ. A more useful interpretation of S can be obtained by rewriting the above relation as

$$S\sim\frac{\delta_s/U_o}{\Delta/U_o} \tag{14}$$

δ_s/U_o represents the time it takes to deform the surface by δ_s with the normal velocity (which scales with U_o) or it is considered to be a measure of the time lag discussed above. Δ/U_o represents the time of convection over Δ, or since the driving force exists mainly over Δ, it is a measure of the time required to change the driving force by convection.

The fact that oscillations appear beyond a certain value of S can be interpreted as follows: One oscillation cycle containing an active period followed by a slow period proceeds. During the active period the surface flow becomes stronger and the center of the recirculation cell moves closer to the cold wall [Fig. 3(a)]. During this period the surface flow is stronger than the return flow so that a certain amount of the fluid is carried away from the hot surface region and is deposited in the cold surface region, which changes the free surface shape in such a way as to build up a pressure field for increasing return flow. Although the return flow always lags behind the surface flow, its cooling becomes increasingly effective since the return flow travels a shorter distance from the cold wall as the cell center moves toward the cold wall. After the increase of the surface flow is reversed, the return flow becomes more dominant than the surface flow and the surface flow recedes to the hot corner as it becomes weaker [Fig. 3(b)]. During this period the fluid accumulates in the hot surface region and is removed from the cold region to change the free surface shape and pressure field in such a way to retard the return flow. At this stage, since the cell center moves toward the hot wall, the amount of the return flow increases [Fig. 3(b)] and only a part of it is directed toward the hot corner because during the slow period less fluid is needed. As the hot corner is nearly isolated from the cooling by the return flow, the surface temperature gradually rises and the next active period starts.

5. Concluding Remarks

From the foregoing analysis one can make the following conclusions regarding the basic thermocapillary flow which is known to become oscillatory: (1) The viscous force dominates over the inertia force and the effect of convection is important in the flow. (2) The flow is driven mainly in the hot corner region.

It is apparent that the free surface deformation plays an important role in oscillatory thermocapillary flow in high Pr fluids. The deformation induces a time lag before the return flow responds to a change in the surface flow and

the parameter S represents the ratio of the time lag to the convection time scale, based on which the oscillation mechanism can be clearly explained.

Reference

Carpenter, B.M. and Homsy, G.M., 1990, "High Marangoni Number Convection in a Square Cavity," *Part II, Physic. Fluids A*, 2, pp. 137~149.

Chen, J.C., Chen, W.C., and Hwu, F.S., 1991, "Numerical Computations of Unsteady Thermocapillary Convection in a Rectangular Cavity with Surface Deformation," *In Heat Transfer in Metals and Containerless Processing and Manufacturing, ASME Publication* HTD-Vol. 162, pp. 89~95.

Chen, J.C. and Chin, G.H., 1995, "Linear Stability Analysis of Thermocapillary Convection in the Floating Zone," J. *Crystal Growth*, Vol. 154, No. 1-2, pp. 98~107.

Chen, Q.S., and Hu, W.R., 1998, "Influence of Liquid Bridge Volume on Instability of Floating Half Zone Convection," *Int. J. Heat Mass Transfer*, Vol. 41, Nos. 6-7, pp. 825~837.

Chun, C.H. and Wuest, W., 1979, "Experiments on the Transition from Steady to the Oscillatory Marangoni Convection of a Floating Zone Under Reduced Gravity Effect," *Acta Astronautica 6*, pp. 1073~1082.

Chun, C.H., 1980, "Experiments on Steady and Oscillatory Temperature Distribution in a Floating Zone Due to the Marangoni Convection," *Acta Astronautica 7*, pp. 479~488.

Kamotani, Y.Ostrach, S. and Vargas, M., 1984, "Oscillatory Thermocapillary Convection in a Simulated Floating Zone Configuration," J. *Crystal Growth* 66, pp. 83~90.

Kamotani, Y. and Lee, K. J., 1989, "Oscillatory Thermocapillary Flow in a Liquid Column Heated by a Ring Heater," *PCH Physico-Chemical Hydrodynamics 11*, pp. 729~736.

Lai, C.L., 1990, "Unsteady Thermocapillary Flows and Free Surface Oscillations in Reduced Gravity Environments," *Acta Astronautica 21*, pp. 171~181.

Lee, J., Lee, D.J., and Lee, J.H., 1995, "On the Mechanism of Oscillation in a Simulated Floating Zone," J. *Crystal Growth*, Vol. 152, pp. 341~346.

Monti, R., 1987, "On the Onset of the Oscillatory Regimes in Marangoni Flows," *Acta Astronautica 15*, pp. 557~560.

Monti, R. and Fortezza, F., 1991, "The Scientific Results of the Experiment on Oscillatory Marangoni Flow Performed in Telescience on Texus 23," *Microgravity Quarterly 1*, pp. 163~171.

Napolitano, L.G., Monti, R., and Russo, G., 1986, "Marangoni Convection in One- and Two-Liquids Floating Zones," *Naturwissenchaften 73*, pp. 352~355.

Ostrach, S., 1977, "Motion Induced by Capillary," *In Physicochemical Hydrodynamics*, V.G. Levich Festschrift 2, pp. 571~589, Advanced Publication.

Ostrach, S., Kamotani, Y., and Lai, C.L., 1985, "Oscillatory Thermocapillary Flows," *PCH Physico-Chemical Hydrodynamics 6*, pp. 585~599.

Patankar, S.V., 1980, Numerical Heat transfer and Fluid Flow, McGraw-Hill.

Preisser, F., Schwabe, D., and Scharmann, A., 1983, "Steady and Oscillatory Thermocapillary Convection in Liquid Columns with Free Cylindrical Surface," J. *Fluid Mech. 126*, pp. 545~567.

Rupp, R., Muller, G., and Neumann, G., 1989, "Three-Dimensional Time Dependent Modeling of the Marangoni Convection in Zone Melting Configurations for GaAs," J. *Crystal Growth 97*, pp. 34~41.

Schwabe, D., Scharmann, A., Preisser, F., and Oeder, R., 1978, "Experiments on Surface Tension Driven Flow in Floating Zone Melting," J. *Crystal Growth 43*, pp. 305~312.

Schwabe, D., Preisser, F., and Scharmann, A., 1982, "Verification of the Oscillatory State of Thermocapillary Convection in a Floating Zone Under Low-Gravity," *Acta Astronautica 9*, pp. 265~273.

Schwabe, D., Velten, R., and Scharmann, A., 1990, "The Instability of Surface Tension Driven Flow in Models for Floating Zones Under Nor-

mal and Reduced Gravity," J. *Crystal Growth 99*, pp. 1258~1264.

Shen, Y., Neitzel, G.P., Jankowski, D.F., and Mittlemann, H.D., 1990, "Energy Stability of Thermocapillary Convection in a Model of the Float-Zone Crystal-Growth Process," J. *Fluid Mech*, 217, pp. 639~660.

Velten, R., Schwabe, D., and Scharmann, A., 1991, "The Periodic Instability of Thermocapillary Convection in Cylindrical Liquid Bridges," *Phys. Fluids A3*, pp. 267~279.

Xu, J-J. and Davis, S.H., 1984, "Convective Thermocapillary Instabilities in Liquid Bridges," *Phys. Fluids 27*, pp. 1102~1107.

Wanschura, M., Shevtsove, V.M., Kuhlmann, H.C., and Rath, H.J., 1995, "Convective Instability Mechanisms in Thermocapillary Liquid Bridges," *Physics Fluids*, Vol. 7, No. 5, pp. 912~925.

Zebib, A., Homsy, G.M., and Meiburg, E., 1985, "High Marangoni Number Convection in a Square Cavity," *Phys. Fluids 28*, pp. 3467~3476.